Progress In Electromagnetics Research M, Vol. 106, 35–46, 2021

A Novel Circular Polarized Rectenna with Wide Ranges of Loads for Wireless Harvesting Energy

Mustapha Bajtaoui*, Otman El Mrabet, Mohammed A. Ennasar, and Mohsine Khalladi

Abstract—In this paper, a novel circularly polarized rectenna, with a harmonic suppression, capable of harvesting low-power RF energy with wide operating output loads is presented. The proposed rectenna is composed of a circularly polarized CPW-fed antenna based on a split ring resonator (SRR) and a wideband rectifying circuit. The circular polarization characteristic is achieved by breaking the symmetry of the SRR. The designed topology is fabricated and measured. Simulated and measured results show that the rectenna's efficiency is more than 45% at 2.45 GHz with an input power of −15 dBm under different polarizations. Importantly, the measured results show that the proposed configuration can maintain the same efficiency over wide ranges of loads (from 1 to 5 kΩ). The measured output dc voltage of the rectifier (without antenna) with a load resistance of 3-kΩ is 0.21 V and 1.22 V at −15 dBm and 0 dBm, respectively. The proposed design concept is very suitable for the 2.45 GHz ISM band (Wi-Fi, Bluetooth, RFID, etc.).

1. INTRODUCTION

In the last decade, Wireless Internet-of-Things (IoT) systems and their related applications have experienced rapid development [1, 2] owing to their huge potential in connecting small devices and the capabilities they provide to make our life smart. Thus, a massive number of IoT devices will be deployed into cities, buildings, connected vehicles, healthcare monitoring, smart shopping, and other environments. In addition, this number of IOT devices is expected to increase in the 5G and 6G technologies era. In such situation, microwave wireless power transfer (WPT) and energy harvesting (EH) technology have attracted much interest in the last decade, which makes the IOT devices more autonomous in terms of energy, thus eliminating the need of batteries or power supply resources due to which their maintenance cost are expensive. In addition, in many circumstances the devices have to be portable, thus wireless power charging is now essential [3, 4].

The rectenna is the cornerstone of the EH and WPT, which consists of four blocks. An antenna that allows to receive a radio frequency (RF) signal and a rectifying circuit is often based on a Schottky diode which converts the RF power to a DC signal across the load (the load represents the input impedance of the device that needs to be powered up), a matching circuit placed between the rectifier and the antenna to maximize the collected power and to prevent the harmonics generated by the diodes from being reradiated by the antenna. The last block is the DC filter placed at the output to smooth the output DC signal [5, 6].

Nowadays, many existing rectenna designs have been reported in the literature [7–13]. However, rectennas presented in references [7–12] were designed to operate in linear polarization which makes them sensitive to incident waves. Thus, the efficiency of energy harvesting system is mainly affected. In order to enhance power collection and hence conversion efficiency, an antenna with circular

Received 21 September 2021, Accepted 11 November 2021, Scheduled 26 November 2021

* Corresponding author: Mustapha Bajtaoui (mustaphabajtaoui@gmail.com).

The authors are with the Electrical Electronics and Microwave Group, Faculty of Science, Abdelmalek Essaadi University, Tetuan 93000, Morocco.

polarization and omnidirectional radiation pattern is well desired because of their abilities to mitigate polarization mismatch and enhance immunity to multipath interferences between transmitting and receiving antennas [14–16]. Furthermore, some reported designs as the one in [7] operate only for one load R_L, hence, the RF to DC conversion may be seriously affected owing to the mismatch between the rectenna and a large number of low power devices with different input impedance values.

In this paper, we propose a circularly polarized rectenna, with a harmonic suppression, which operates in a low-power RF energy with wide operating output loads. The circular polarization is achieved by breaking the symmetry of the split ring resonator (SRR) in order to maintain the value of the output power constant for all directions. The remainder of this paper is organized as follows. Section 2 presents the design, fabrication, and measurements results of the circularly polarized antenna. Next, the design and measurements of the fabricated rectifier are given in Section 3. Section 4 presents the measurement results of the rectenna system (antenna + rectifier). Finally, Section 5 draws some conclusions.

2. CIRCULAR POLARIZED ANTENNA

In this section, a circularly polarized antenna based on an SRR to collect the RF energy at 2.45 GHz is presented. The proposed design characteristics are optimized by using a transient domain solver within the commercial software package CST Microwave Studio [17]. The physical geometry of the proposed antenna is shown in Figure 1. It is printed on a Rogers RT/Duroid 6002 substrate of permittivity $\varepsilon_r = 2.93$, loss tangent of 0.0012, and thickness of $h = 1.58\,\text{mm}$ with a single side copper cladding of 35 µm. The overall size of the substrate is $60 \times 40\,\text{mm}^2$, which is $0.49\lambda_0 \times 0.32\lambda_0$ at 2.45 GHz. A Coplanar Waveguide (CPW) feeding technique with 50-Ω transmission line was used to excite the SRR. It is worthwhile to mention that the proposed design can be fabricated easily with standard PCB manufacturing technologies and with lower cost. The width and slot of the 50-Ω CPW feed line are chosen to be $w_f = 4.5\,\text{mm}$ and $G_1 = 0.3\,\text{mm}$, respectively.

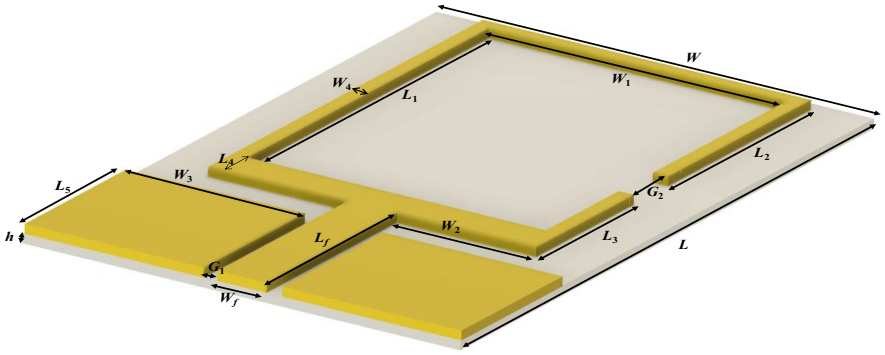

Figure 1. Schematic configuration of the proposed circular polarized antenna.

The optimized parameters of the SRR along with other parameters of the antenna are listed in Table 1. These dimensions have been selected to place the quasi-static resonance within the S-band of the microwave spectrum according to the theory developed in [18], based on the excitation of quasi-static resonance of the SRR element, provided by magnetic field component supported by the CPW transmission line.

The design process of the proposed configuration starts with a simple CPW feeding. Then, a symmetric SRR is attached to the CPW feed line which allows to excite the quasi-static resonance of the SRR. Finally, the gap (G_2) has been displaced gradually, as shown in Figure 2, to check its effect on the reflection coefficient and on the axial ratio. The simulated transmission coefficient and axial ratio as a function of frequency for the four configurations, which simply differ by the position of the gap in the ring, are plotted in Figure 3.

From Figure 3, we can see clearly that the reflection coefficient and axial ratio are much sensitive

Table 1. Geometrical parameters of the proposed CP antenna.

Parameter	Value (mm)	Parameter	Value (mm)	Parameter	Value (mm)
w	40	w_f	4.5	L_4	3.6
w_1	27.2	L	60	L_5	11
w_2	12.75	L_1	35.1	L_f	19
w_3	17.45	L_2	19	G_1	0.3
w_4	1.4	L_3	13.6	G_2	7.5

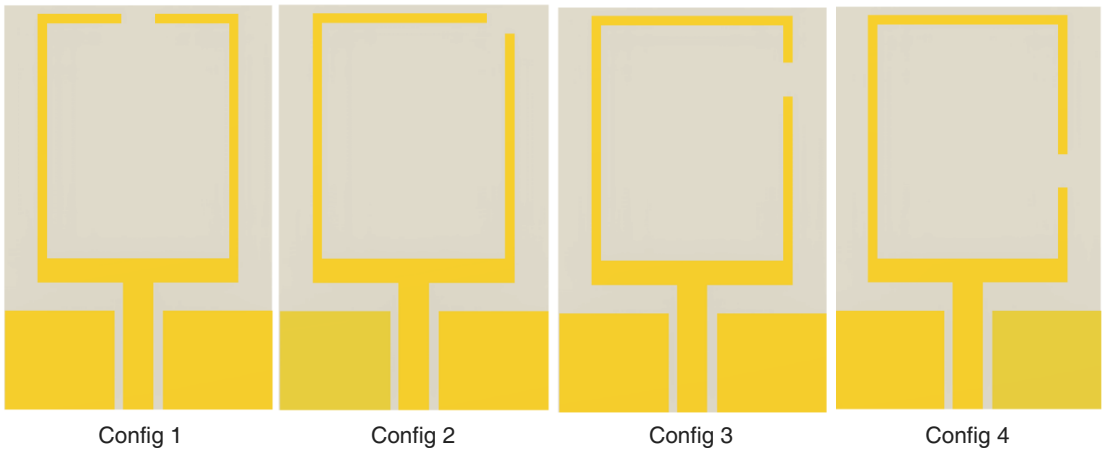

Figure 2. Design evolution of the proposed design.

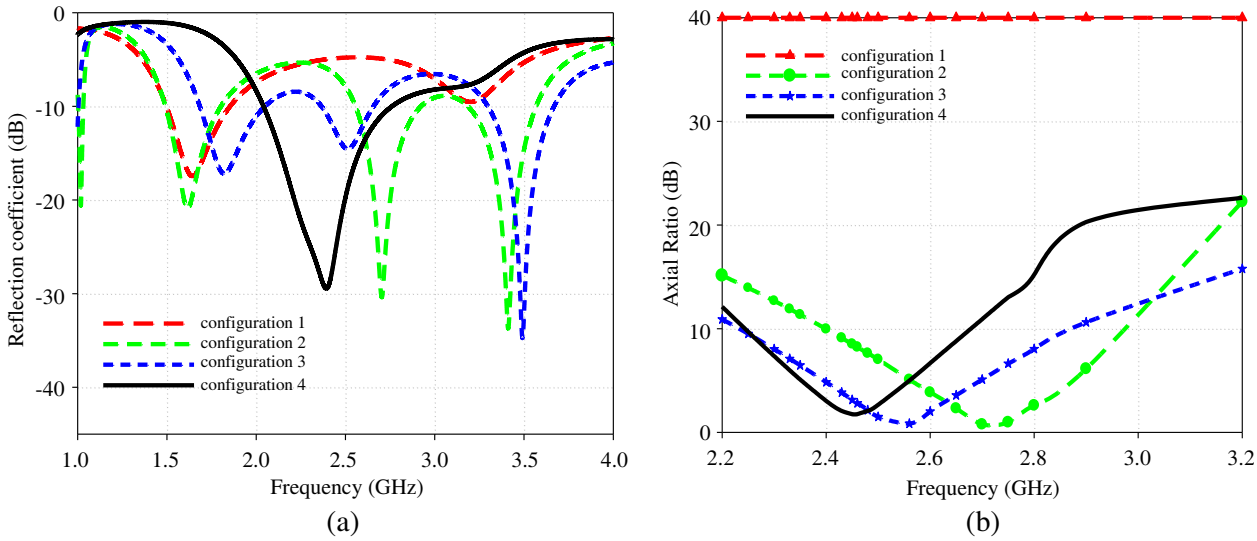

Figure 3. Simulated curves of the reflection coefficient and axial ratio of four configurations of the monopole antenna. (a) Reflection coefficient. (b) Axial ratio.

to the shift of the gap. In particular, it is demonstrated that the resonance and axial ratio (AR) can be properly controlled by varying the position of the gap. Figure 3(a) shows that for configuration I, one resonance is observed around 1.5 GHz. When moving the gap (configuration II and III), we interestingly find that the antenna exhibits three resonances. Moreover, when the displacement is further enlarged

(configuration IV) a wideband resonance located around 2.45 GHz is achieved. On the other hand, Figure 3(b) shows that the axial ratio of the configuration I is close to 40 dB, indicating a highly linear polarization. After moving the gap, the axial ratio of the other configurations is reduced to less than 3 dB over the entire impedance bandwidth.

The circular polarization is achieved by combining two orthogonal transmission modes at the same frequency with equal amplitude and a 90° phase difference, which is created by moving the gap as shown in Figure 2. To give more physical insight into the circular polarization capability, the current distributions in the $+z$-direction at the resonant frequency 2.45 GHz for four different time phases ($\omega t = 0°$, $\omega t = 90°$, $\omega t = 180°$, and $\omega t = 270°$) are illustrated in Figure 4. We can see clearly that the dominant surface current along x-direction at $\omega t = 0°$ is perpendicular to the one along $+y$ direction at $\omega t = 90°$, which satisfies the requirement of the spatial and temporal quadrature for circular polarization. In addition, Figure 4 reveals that the surface currents at $\omega t = 180°$ and $\omega t = 270°$ are equal in magnitude and opposite in phase of $\omega t = 0°$ $\omega t = 90°$. We can also see that with the increment of time by $t/4$, the surface currents rotate in clockwise direction and hence generate a right hand circular polarization (RHCP) in the $+z$-direction, whereas an LHCP is produced for $-z$ direction [19].

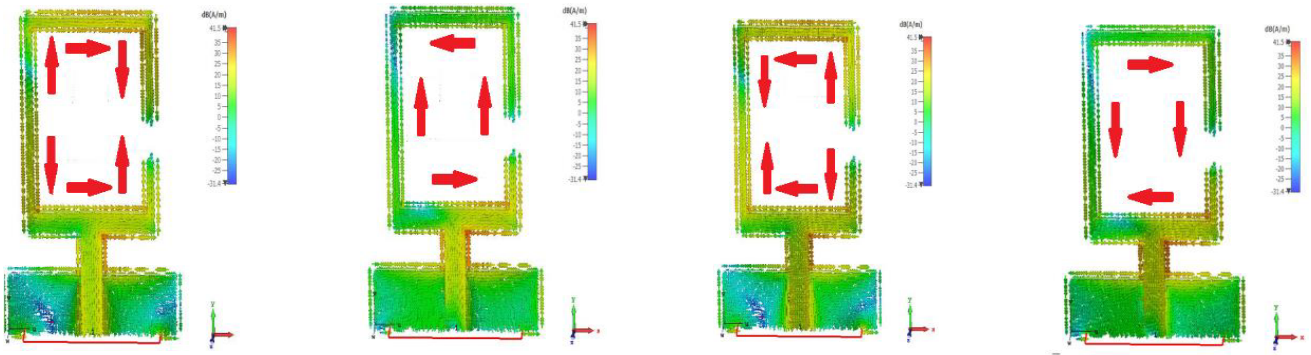

Figure 4. Simulated current distribution. (a) 0°, (b) 90°, (c) 180° and (d) 270°.

To confirm the above numerical results, the optimized antenna (configuration IV) has been fabricated using an LPKF Protomat S100 mill/drill unit, as show in Figure 5(a), and its performance has been characterized experimentally. Figure 5(b) presents the simulated and measured reflection coefficients of the proposed design as a function of the frequency. We measured the reflection coefficient of the prototype using a vector network analyzer (Agilent N5222A PNA).

We can see a good agreement between measured and simulated results. The simulated reflection coefficient is −25 dB at 2.45 GHz, with a bandwidth (S_{11} less than −10 dB) of 700 MHz. However, the measured reflection coefficient is −19 dB at 2.45 GHz with the bandwidth (S_{11} less than −10 dB) of 420 MHz. The small discrepancy between simulated and measured results can be ascribed to the fabrication tolerances. It is worthwhile to mention that the proposed configuration can be designed to fulfill the requirement of different wireless communication systems just by varying the geometrical parameters (L_1, W_1) of the split ring resonator (SRR). Figure 6(a) provides a view of a 3D simulated radiated pattern, and Figures 6(b) and 6(c) show the simulated and measured radiation patterns of the antenna at 2.45 GHz for E- and H-planes. Despite the slight deviation between the simulation and measurement, the two results are in good agreement, and a monopole like radiation patterns is obtained.

The simulated radiation efficiency of the antenna is presented in Figure 7(a). We can see clearly that at 2.45 GHz the radiation efficiency is near 89%. We have also measured the gain of the proposed antenna. The obtained results are depicted in Figure 7(b). There is a good agreement between simulation and measurements results. The measured peak gain of 2.1 dBi is observed for the antenna at the central operating frequency of 2.45 GHz.

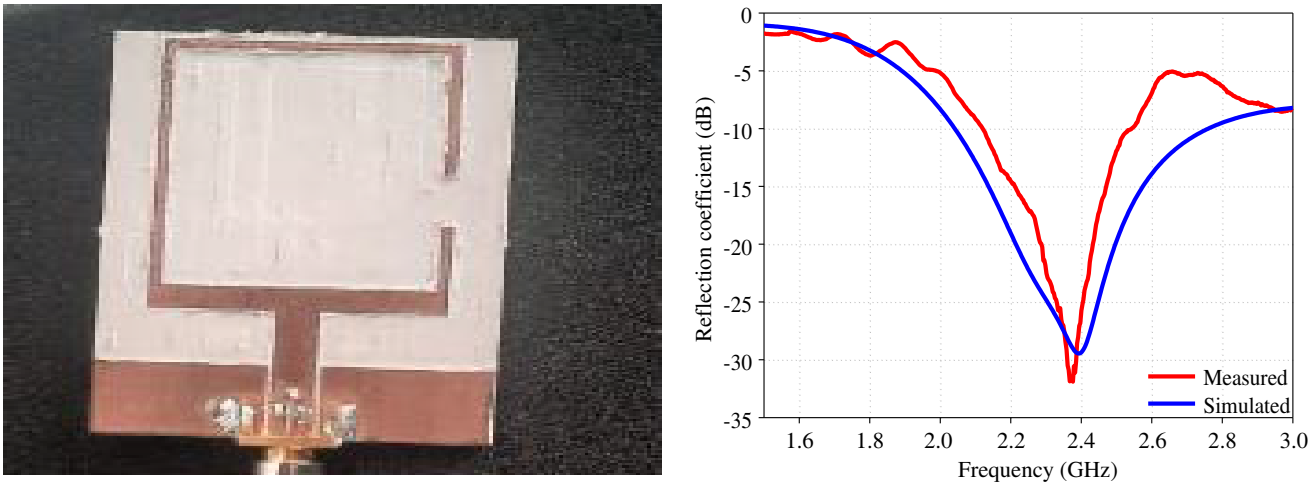

(a) (b)

Figure 5. (a) Photo of the fabricated antenna. (b) Simulated and measured reflection coefficient of the proposed antenna.

3. RECTIFYING CIRCUIT DESIGN

This section primarily focuses on the design and optimization of the rectifying circuit used for the proposed rectenna configuration. Generally, the rectifier consists of one or more Schottky diodes (non-linear device that generates harmonics), a matching network placed before diode Schottky that has two scopes: having a maximum power provided by the antenna to the rectifier and prevents any harmonics from the diodes being reradiated. Finally, a DC-pass filter smoothes the ripple of DC output. Single-diode structures are the most used for low input power levels [20]. Thus, the rectifying circuit designed for this work is based on zero bias Schottky diode (SMS7630-079LF) [21] in SOT-23 which is most appropriate for low RF input power applications. This Schottky diode has small parasitic effects that are modeled by a capacitance in parallel C_P and an inductance L_P in series, and their values are 0.185 pF and 0.7 nH, respectively. The main aim of the proposed rectenna is to be able to feed several electronic devices (rectifier load) at low power (around -15 dBm). However, the input impedance of those devices varies from one device to another. Therefore, the challenge is to achieve a matching circuit over wide load power ranges, which allow us to have an almost flat maximum efficiency. The presented circuit shown in Figure 8(a) is designed using ADS circuit simulator software. First, the Large Signal S-Parameter (LSSP) simulation with a parameter sweep in ADS was used to convert the input impedance of the rectifier $(16 - j167)\,\Omega$ to 50-Ω, and therefore get the reflection coefficient at the operating frequency. Then, Harmonic Balance (HB) simulation was performed to take into account the nonlinearity of the Schottky diode, and finally the harmonic balance and Momentum tools are used for co-simulation to get accurate results. The rectifying circuit is printed on a RO5880 substrate with $\varepsilon_r = 2.33$ and 0.8 mm thickness. The optimized rectifying circuit was fabricated, as shown in Figure 8(b).

Simulated and measured reflection coefficients of the rectifying circuitry for the input power signal level of -15 dBm is depicted in Figure 9(a). The simulated and measured results match well with each other. Furthermore, the measurements show that the rectifier is well adapted at 2.45 GHz for input power -15 dBm with a selected load of 3 kΩ. For the second and third harmonics (not shown here), a mismatch in the measured values is observed with S_{11} close to 0.08 dB and 0.14 dB at 4.9 GHz and 7.35 GHz, respectively. We have also measured the reflection coefficient of the rectifying circuitry for different input power values, which are depicted along with simulated results in Figure 9(b). As in Figure 9(a), we can see a good matching between simulated and measured results. Figure 9(b) reveals that our rectifying circuit remains well matched up to -5 dBm.

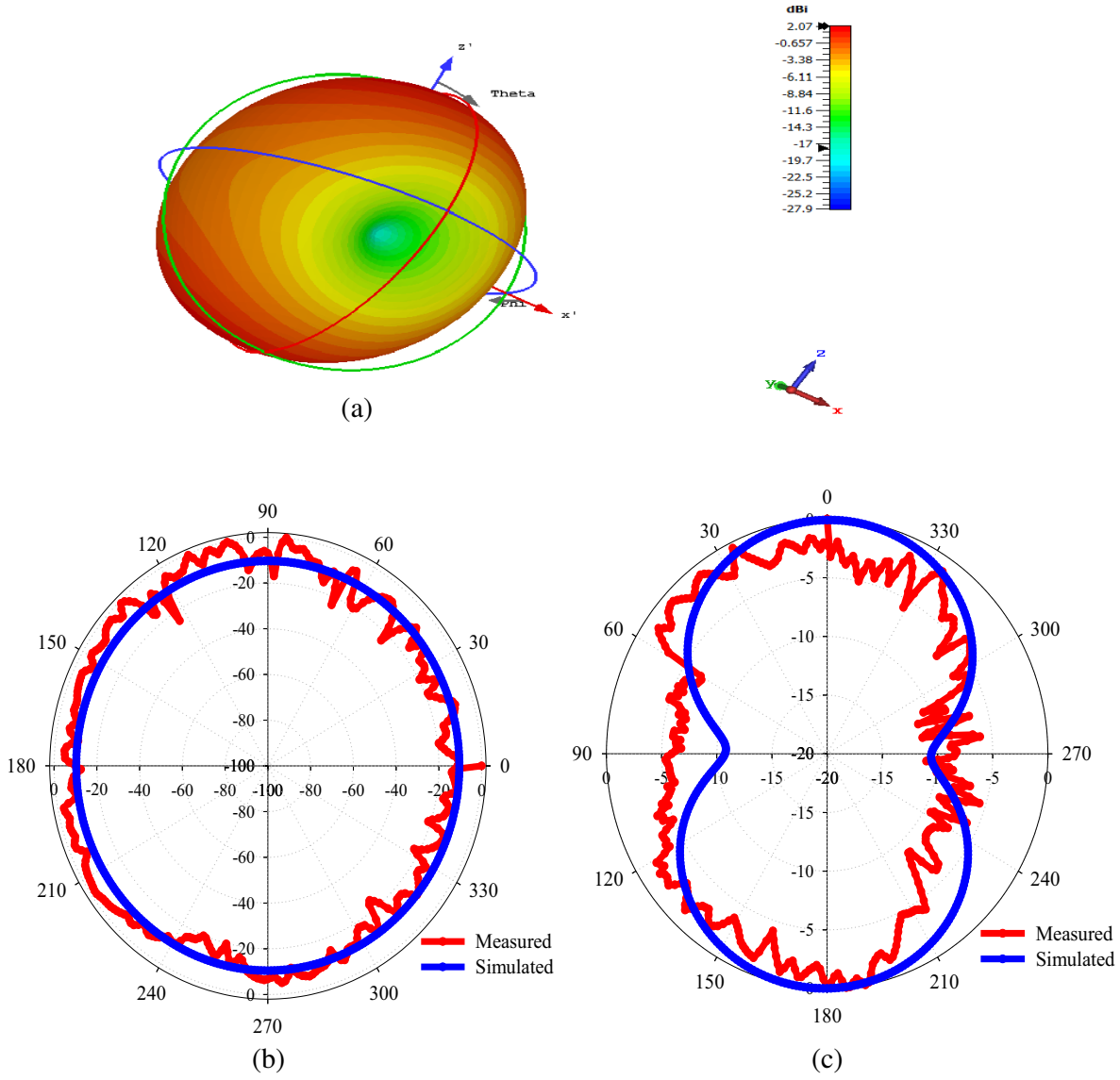

Figure 6. Simulated and measured radiation patterns of the proposed antenna at 2.45 GHz, (a) 3D, (b) E-plane, (c) H-plane.

Next, we have measured the efficiency of the rectifying circuit, which can be calculated as follows:

$$\eta = \frac{P_{\mathrm{DC_{out}}}}{P_{\mathrm{RF_{in}}}} * 100 = \frac{V_{\mathrm{out}}^2}{R_{\mathrm{DC}}} * \frac{1}{P_{\mathrm{RF_{in}}}} * 100 \tag{1}$$

where $P_{\mathrm{DC_{out}}}$ is the output dc power, V_{out} the measured dc voltage across the load, and $P_{\mathrm{RF_{in}}}$ the RF power available at the input of the rectifying circuit. The experimental setup for measuring the efficiency of the rectifying circuit is given in Figure 10.

The RF power $P_{\mathrm{RF_{in}}}$ is generated by a signal generator from Rhode Schwartz SMF 100A which is connected to the rectifying circuit via an SMA connector. The output of the rectifying circuit is connected to a variable resistor. The dc voltage across the load V_{out} is measured using a multimeter. Figure 11(a) presents the measured and simulated RF to DC efficiencies of the rectifying circuit at 2.45 GHz for different received input powers (P_{in}), and Figure 11(b) shows the measured and simulated output voltages and output DC powers as a function of the input power (P_{in}) for a load of 3-kΩ. There is a good agreement between simulation and measurements. Also, it is noted that the RF to DC efficiency is above 45% in a wide range of received power.

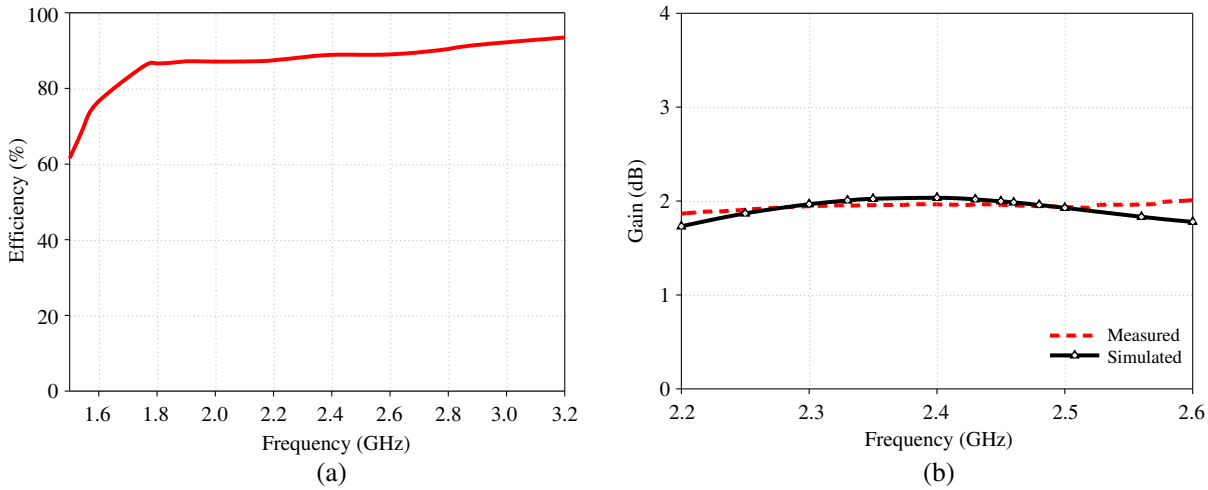

Figure 7. (a) Simulated radiation efficiency of the antenna. (b) Simulated and measured realized gain of the proposed antenna.

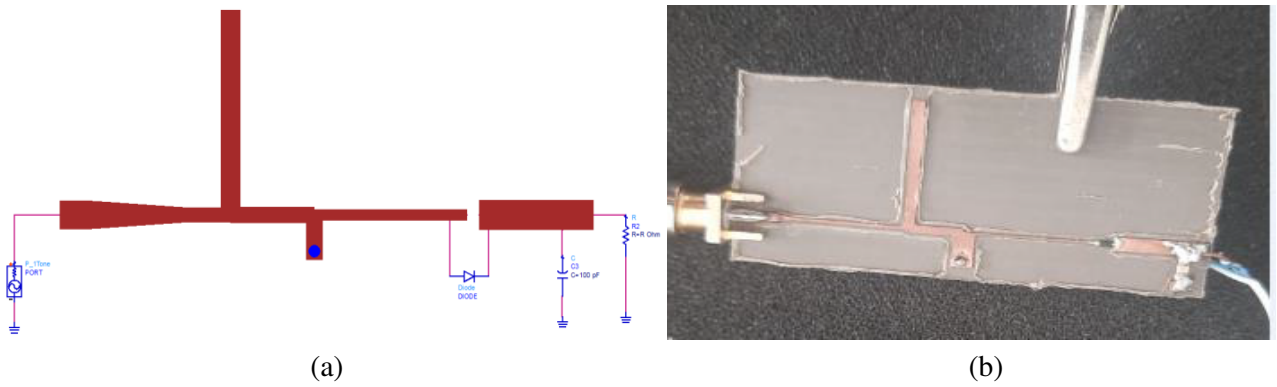

Figure 8. (a) Designed schematic of the rectifier. (b) Fabricated rectifying circuit.

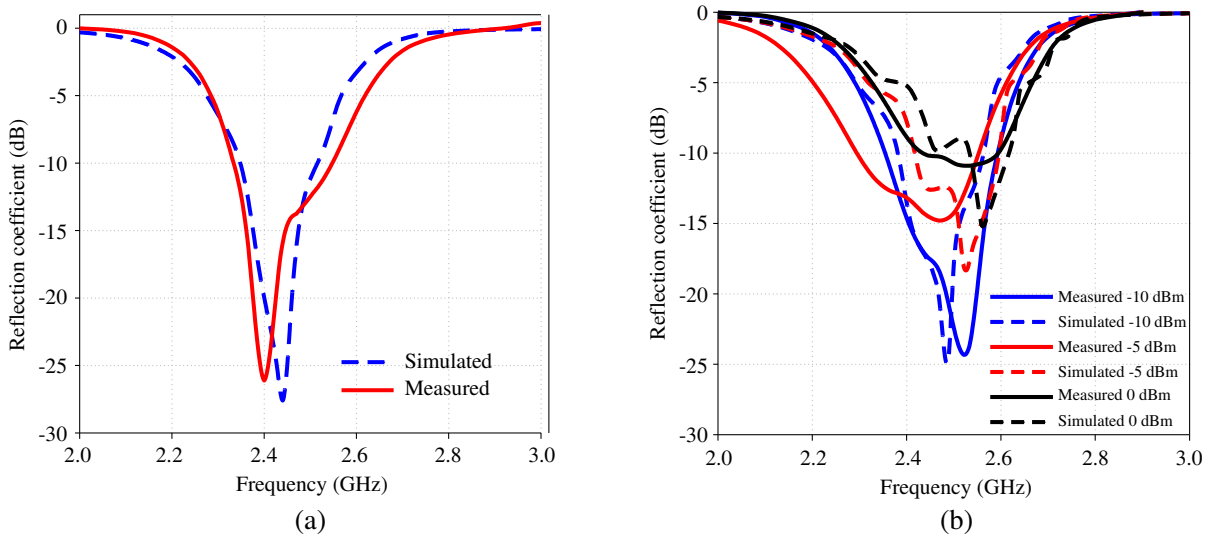

Figure 9. (a) The simulated and measured reflection coefficient at 2.45 for $p_{\text{in}} = -15\,\text{dBm}$. (b) The simulated and measured reflection coefficient versus frequency at different input power levels.

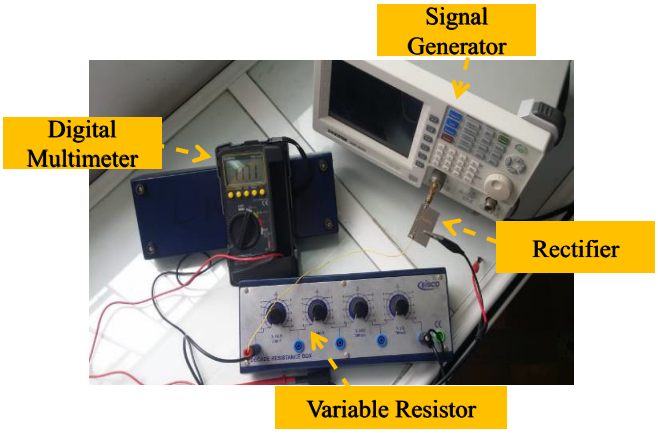

Figure 10. Efficiency measurement setup of the rectifying circuit in free space.

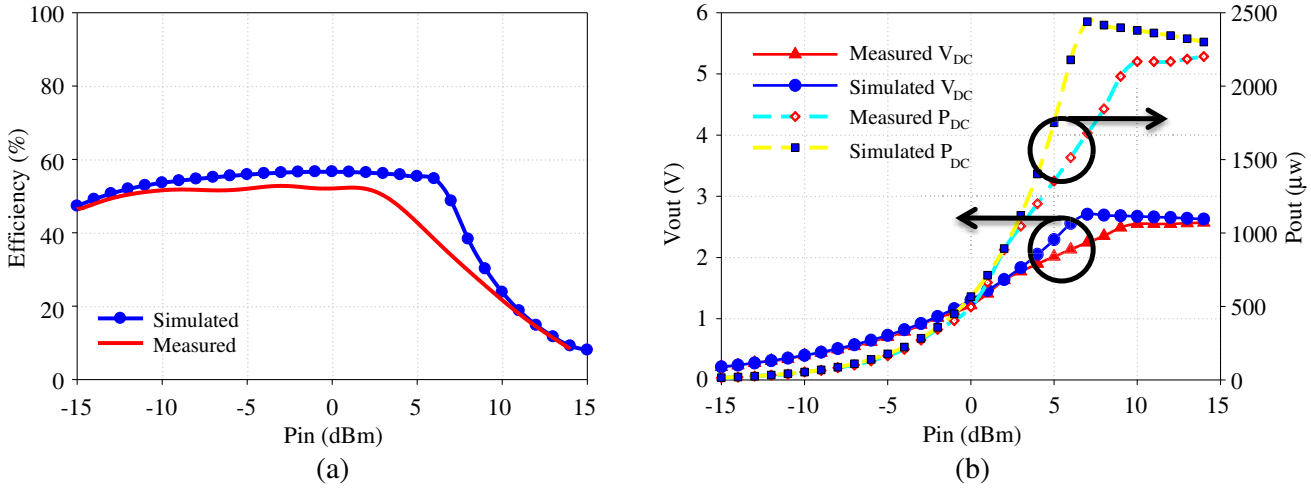

Figure 11. (a) Simulated and measured RF to dc conversion efficiency of the rectifying circuit and (b) DC output (voltage and power).

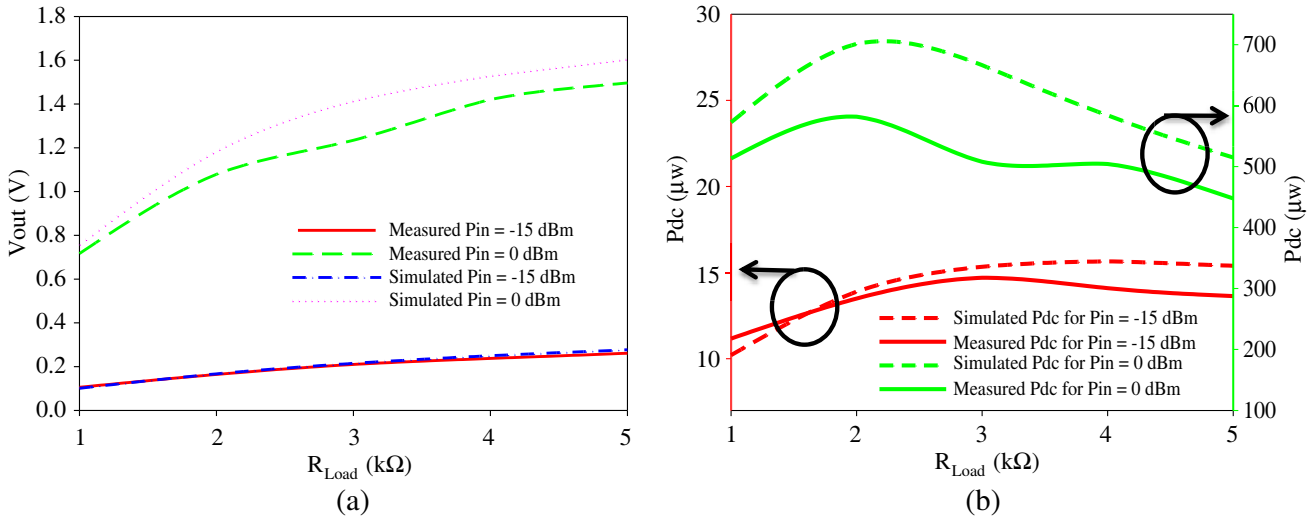

Figure 12. DC output versus load for input power −15 dBm and 0 dBm. (a) Voltage. (b) Power.

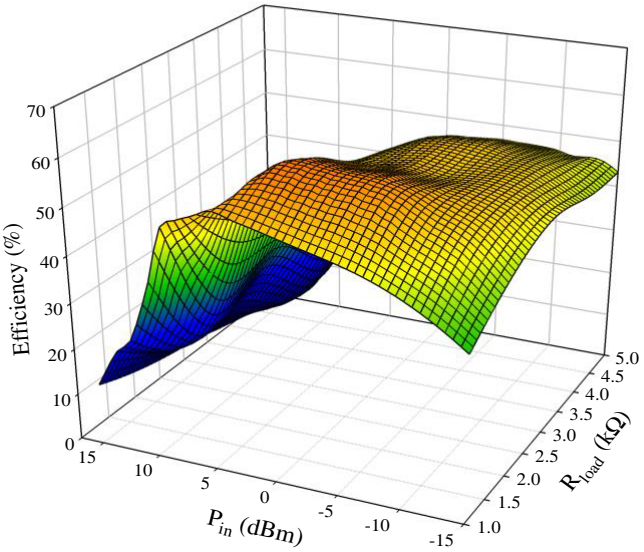

Figure 13. The measured 3D rectifier efficiency as a function of input power and output load.

From Figure 11(b), the measured output voltage of the rectifier is 0.21 V (14.7 µW) and 1.22 V (496 µW) at −15 dBm and 0 dBm, respectively.

Figures 12(a) and (b) illustrate the DC output voltage and DC output power for different values of the load R_L, respectively for $P_{\text{in}} = -15\,\text{dBm}$ and $P_{\text{in}} = 0\,\text{dBm}$.

From Figure 12, we can see that the DC output varies slightly with the variation of the load. These results demonstrate that the rectifier works for a wide range of load under low input power levels.

Figure 13 shows the measured and simulated efficiencies versus input power (P_{in}) and output load (R_{Load}), and the maximum efficiency is 60% at $P_{\text{in}} = 2\,\text{dBm}$ and $R_{\text{Load}} = 2\,\text{k}\Omega$.

4. RECTENNA MEASUREMENTS

The CP antenna and rectifying circuit presented in the above paragraphs are combined to form a single rectenna. Note that the CP antenna and rectifying circuit are integrated over two different substrates, and the connection is assured via an SMA adapter. The rectenna was measured in free space using the measurement kit shown in Figure 14. It consists of an ultra-wideband (UWB) Double-Ridged TEM

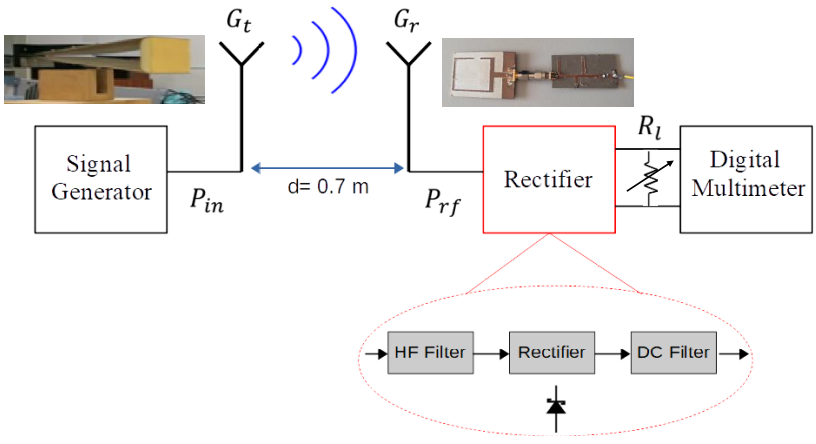

Figure 14. Schematic of the measurement set-up in free space.

linear polarized horn antenna with Lens (2 GHz–26 GHz) to emit the electromagnetic power generated from an RF signal source from Rhode Schwartz, to the rectenna. The realized gain of this linearly polarized horn antenna is approximately 6 dBi at 2.45 GHz. The LP horn antenna is connected to RF signal source via a coaxial cable having a total loss of 2 dB at 2.45 GHz. The rectenna was placed 0.7 m away from the LP horn antenna, which is in the far-field region of the LP horn antenna, that is, greater than 0.55 m at 2.45 GHz according to the $2D^2/\lambda_0$ value. The output dc voltage V_{out} of the rectenna was measured with a multimeter. Note that the spectrum analyzers with our CP antenna have been used to measure the collected power (in this case −15 dBm) at a specific frequency of interest (2.45 GHz).

By measuring the output voltage V_{out} (across the load resistance), the efficiency of the rectenna can be calculated using Equation (1). The rectenna efficiency as a function of the load with input power level −15 dBm at 2.45 GHz frequency is depicted in Figure 15. It can be seen that when the load is around 3-kΩ, the rectenna has a maximum efficiency close to 46% for −15 dBm input power. Note that the measured efficiency is above 30% in a wide range of loads (from 1 to 5 kΩ).

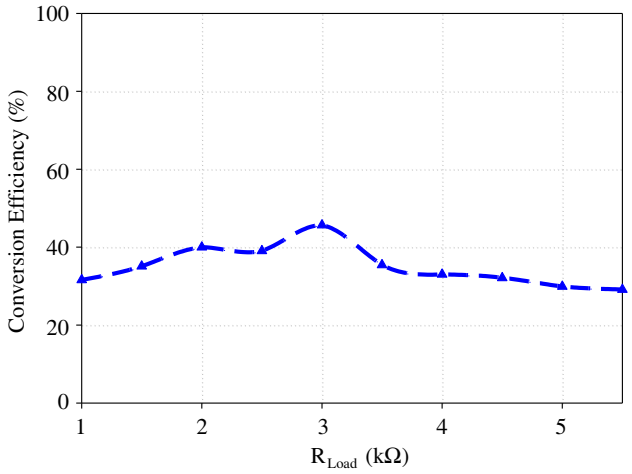

Figure 15. Measured efficiency of the rectenna as a function of load with input power level −15 dBm at 2.45 GHz.

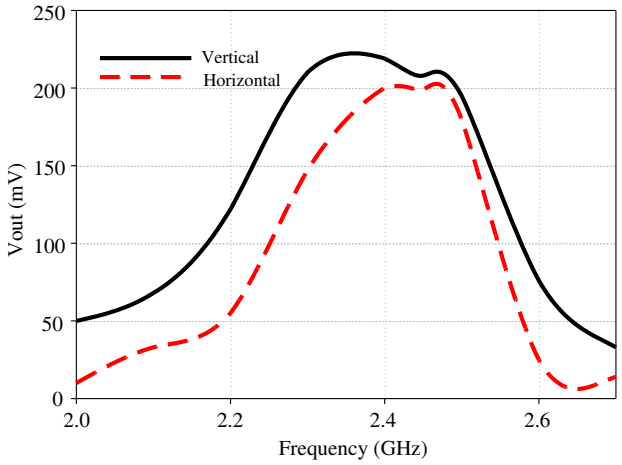

Figure 16. Measured output DC voltage under two different for two rectenna's positions (Vertical: 0° and horizontal: 90°) under input power level −15 dBm.

To check that our rectenna remains capable of capturing electromagnetic waves regardless of their orientations, owing to the use of a circularly polarized antenna, we have conducted other measurements by varying the positions of the rectenna. For the sake of simplicity, we have measured V_{out} for two rectenna's positions (Vertical: 0° and Horizontal: 90°). The obtained results are shown in Figure 16. It can be clearly seen that V_{out} remains more or less constant for both positions, which means that the proposed circularly polarized rectenna provides a stable efficiency regardless of its rotation angle.

Table 2. Comparison of the proposed rectenna with some previously reported rectennas in the literature.

Reference	Input power (dBm)	Efficiency (%)	Antenna polarization	Rectenna Size (mm^2)
[9]	−15	26.5–28	Linear	40 × 33
[10]	−17.5	50	—	3D
[12]	−9	30	Linear	3D
[13]	−15	41.4	Circular	100 × 110
This work	−15	46	Circular	114 × 40

A comprehensive comparison between previously reported rectennas and ours in terms of efficiency, polarization type, and electrical size is summarized in Table 2. It can be observed that the proposed rectenna has a low profile and easy fabrication while having a good efficiency for low incident RF power densities.

5. CONCLUSIONS

In this paper, a design of a new 2.45 GHz rectenna with circular polarization capability has been proposed. The obtained results show that the proposed rectenna can work at low-input RF power with wide operating output loads. The overall rectenna dimension is only $110 \times 40 \times 1.6\,\text{mm}^3$, which is smaller than other previously reported work related to RF energy harvesting applications, while it still shows good performance.

Indeed, the measurement results indicate that the maximum dc voltage at 2.45 GHz is about 2.5 V, and the resulting dc power and RF to DC conversion efficiency are 14.42 µW and 45.60%, respectively, with an incident power density of $1.634\,\mu\text{W/cm}^2$ ($p_{\text{in}} = -15\,\text{dBm}$ gain of antenna 2.1 dBi) at the rectenna location. The proposed circularly polarized rectenna can be used to supply a wide variety of low power wireless electronic systems, which are used in a huge number of applications such as patient in-home health monitoring.

REFERENCES

1. Pandey, R., A. K. Shankhwar, and A. Singh, "An improved conversion efficiency of 1.975 to 4.744 GHz rectenna for wireless sensor applications," *Progress In Electromagnetics Research C*, Vol. 109, 217–225, 2021.
2. Lin, W. and R. W. Ziolkowski, "Wirelessly powered internet-of-things sensors facilitated by an electrically small Egyptian axe dipole rectenna," *Asia-Pacific Microwave Conference Proceedings, APMC*, 891–892, Dec. 2019, doi: 10.1109/APMC46564.2019.9038497.
3. Okba, A., A. Takacs, and H. Aubert, "Compact flat dipole rectenna for IoT applications," *Progress In Electromagnetics Research C*, Vol. 87, 39–49, 2018.
4. Carvalho, A., N. Carvalho, P. Pinho, and R. Gonçalves, "Wireless power transmission and its applications for powering Drones," *8th Congress of the Portuguese Committee of URSI*, 2014.
5. Takhedmit, H., L. Cirio, F. Costa, and O. Picon, "Transparent rectenna and rectenna array for RF energy harvesting at 2.45 GHz," *8th European Conference on Antennas and Propagation, EuCAP 2014*, 2970–2972, 2014, doi: 10.1109/EuCAP.2014.6902451.
6. Takhedmit, H., Z. Saddi, and L. Cirio, "A high-performance circularly-polarized rectenna for wireless energy harvesting at 1.85 and 2.45 GHz frequency bands," *Progress In Electromagnetics Research C*, Vol. 79, 89–100, 2017.
7. Lu, P., X. S. Yang, J. L. Li, and B. Z. Wang, "A compact frequency reconfigurable rectenna for 5.2- and 5.8-GHz wireless power transmission," *IEEE Trans. Power Electron.*, Vol. 30, No. 11, 6006–6010, Nov. 2015, doi: 10.1109/TPEL.2014.2379588.
8. Li, X., L. Yang, and L. Huang, "Novel design of 2.45-GHz rectenna element and array for wireless power transmission," *IEEE Access*, Vol. 7, 28356–28362, 2019, doi: 10.1109/ACCESS.2019.2900329.
9. Palazzi, V., et al., "Design of a ultra-compact low-power rectenna in paper substrate for energy harvesting in the Wi-Fi band," *2016 IEEE Wireless Power Transfer Conference (WPTC)*, Aveiro, Portugal, Jun. 2016, doi: 10.1109/WPT.2016.7498823.
10. Sun, H., Y. X. Guo, M. He, and Z. Zhong, "Design of a high-efficiency 2.45-GHz rectenna for low-input-power energy harvesting," *IEEE Antennas Wirel. Propag. Lett.*, Vol. 11, 929–932, 2012, doi: 10.1109/LAWP.2012.2212232.
11. Olgun, U., C. Chen, and J. L. Volakis, "Investigation of rectenna array configurations for enhanced rf power harvesting," *IEEE Antennas Wirel. Propag. Lett.*, Vol. 10, 262–265, 2011, doi: 10.1109/LAWP.2011.2136371.

12. Niotaki, K., S. Kim, S. Jeong, A. Collado, A. Georgiadis, and M. M. Tentzeris, "A compact dual-band rectenna using slot-loaded dual band folded dipole antenna," *IEEE Antennas Wirel. Propag. Lett.*, Vol. 12, 1634–1637, 2013, doi: 10.1109/LAWP.2013.2294200.
13. Haboubi, W., H. Takhedmit, J.-D. Lan Sun Luk, S.-E. Adami, B. Allard, F. Costa, C. Vollaire, O. Picon, and L. Cirio, "An effcient dual-circularly polarized rectenna for RF energy harvesting in the 2.45 GHz ISM band," *Progress In Electromagnetics Research*, Vol. 148, 31–39, 2014.
14. Bao, X., K. Yang, O. O'Conchubhair, and M. J. Ammann, "Differentially-fed omnidirectional circularly polarized patch antenna for RF energy harvesting," *2016 10th European Conference on Antennas and Propagation (EuCAP)*, Davos, Switzerland, May 2016, doi: 10.1109/EuCAP.2016.7481820.
15. Cao, Y., W. Hong, L. Deng, S. Li, and L. Yin, "A 2.4 GHz circular polarization rectenna with harmonic suppression for microwave power transmission," *Proceedings — 2016 IEEE International Conference on Internet of Things; IEEE Green Computing and Communications; IEEE Cyber, Physical, and Social Computing; IEEE Smart Data, iThings-GreenCom-CPSCom-Smart Data 2016*, 359–363, May 2017, doi: 10.1109/iThings-GreenCom-CPSCom-SmartData.2016.85.
16. Huang, F. J., T. C. Yo, C. M. Lee, and C. H. Luo, "Design of circular polarization antenna with harmonic suppression for rectenna application," *IEEE Antennas Wirel. Propag. Lett.*, Vol. 11, 592–595, 2012, doi: 10.1109/LAWP.2012.2201437.
17. "CST Studio Suite 3D EM simulation and analysis software," https://www.3ds.com/products-services/simulia/products/cst-studio-suite/?utm_source=cst.com&utm_medium=301&utm_campaign=cst (accessed May 27, 2021).
18. Marqués, R., F. Mesa, J. Martel, and F. Medina, "Comparative analysis of edge- and broadside-coupled split ring resonators for metamaterial design — Theory and experiments," *IEEE Trans. Antennas Propag.*, Vol. 51, No. 10, 2572–2581, Oct. 2003, doi: 10.1109/TAP.2003.817562.
19. "145-2013 — IEEE Standard for Definitions of Terms for Antennas/IEEE Standard/IEEE Xplore," https://ieeexplore.ieee.org/document/6758443 (accessed Mar. 31, 2021).
20. Mabrouki, A., M. Latrach, and V. Lorrain, "High efficiency low power rectifier design using zero bias schottky diodes," *2014 IEEE Faible Tension Faible Consommation*, Monaco, Monaco, 2014, doi: 10.1109/FTFC.2014.6828604.
21. Skyworks, "Surface mount mixer and detector schottky diodes data sheet, document #200041," accessed: Mar. 31, 2021, [online], available: www.skyworksinc.com.